

# Nuclear expansion and symmetry energy of hot nuclei

D.V. Shetty\*, G.A. Souliotis, S. Galanopoulos, Z. Kohley,  
S.N. Soisson, B.C. Stein, S. Wuenschel, and S.J. Yennello,

*Cyclotron Institute, Texas A&M University, College Station, TX 77843, USA*

---

## Abstract

The decrease in the symmetry energy of hot nuclei populated in  $^{58}\text{Ni} + ^{58}\text{Ni}$ ,  $^{58}\text{Fe} + ^{58}\text{Ni}$  and  $^{58}\text{Fe} + ^{58}\text{Fe}$  reactions at beam energies of 30, 40 and 47 MeV/nucleon, as a function of excitation energy is studied. It is observed that this decrease is mainly a consequence of increasing expansion or decreasing density rather than the increasing temperature. The results are in good agreement with the recently reported microscopic calculation based on the Thomas-Fermi approach. An empirical relation to study the symmetry energy of finite nuclei in various mass region is proposed.

*Key words:* Symmetry energy; Excitation energy; Nuclear expansion; Hot nuclei  
*PACS:* 21.65.Ef; 25.70.Pq; 21.65.Mn

---

The symmetry energy, which is the difference in energy per nucleon between the pure neutron matter and the symmetric nuclear matter, is a topic of significant interest [1]. Traditionally, the symmetry energy coefficient of nuclei has been extracted by fitting the binding energy in their ground state with various versions of the liquid drop mass formula [2]. The properties of nuclear matter are then determined by theoretically extrapolating the nuclear models designed to study the structure of real nuclei. However, real nuclei are cold ( $T \approx 0$  MeV), nearly symmetric ( $N \approx Z$ ) and found at equilibrium density ( $\rho_0 \approx 0.16 \text{ fm}^{-3}$ ). It is not known how the symmetry energy evolves at temperatures and densities away from normal nuclear conditions. In particular, the density and the energy dependence of the symmetry energy are actively being sought. Information on the symmetry energy as a function of density and temperature is crucial for many astrophysical calculations such as, determining the

---

\* Corresponding author  
*Email address:* shetty@comp.tamu.edu.

structure and cooling of neutron stars, and simulating the dynamics of supernova collapse [3]. It is also important in studies related to the structure of neutron-rich nuclei, where it is known to be intimately related to the neutron skin thickness [4].

The disassembly of a hot nucleus into several light and heavy fragments in a process called multifragmentation [5,6,7] provides an important means of studying nuclei away from normal nuclear conditions. Over the last several decades many measurements have been carried out. Some of the important results that have emerged from these studies are: i) The temperature of the hot nucleus increases rapidly with increasing excitation energy, until a near flattening or a plateau-like region appears at higher excitation energy where the temperature remains fairly constant (*caloric curve*) [8]. ii) The density of the hot nucleus decreases as the excitation energy increases [9,10] due to thermal expansion. iii) The symmetry energy, obtained from the yield distribution of the fragments following the disassembly of hot nuclei, is significantly lower than those normally assumed in various model calculations [11,12,13,14].

Currently, there exist no detailed understanding of how the symmetry energy evolves with the excitation energy of hot nuclei. In this work, we examine the excitation energy dependence of the symmetry energy in multifragmentation of hot nuclei ( $A \sim 100$ ) populated in  $^{58}\text{Ni} + ^{58}\text{Ni}$ ,  $^{58}\text{Fe} + ^{58}\text{Ni}$  and  $^{58}\text{Fe} + ^{58}\text{Fe}$  reactions, and propose an empirical relation for studying the symmetry energy in various mass regions.

It is known that in multifragmentation reaction, the ratio of fragment isotopic yields from two different reactions, 1 and 2,  $R_{21}(N, Z)$ , follows an exponential dependence on the fragment neutron number ( $N$ ) and the proton number ( $Z$ ); an observation known as isoscaling [7,15,16]. The dependence is characterized by a simple relation given as,

$$R_{21}(N, Z) = Y_2(N, Z)/Y_1(N, Z) = C \cdot \exp(\alpha N + \beta Z), \quad (1)$$

where  $Y_2$  and  $Y_1$  are the fragment yields from the neutron-rich and neutron-deficient systems, respectively.  $C$  is an overall normalization factor, and the quantities  $\alpha$  and  $\beta$  are the isoscaling parameters.

For the present study, we make use of the experimentally determined fragment yield distribution and the isoscaling parameter  $\alpha$ , obtained from the above scaling relation, for two different pairs of reactions,  $^{58}\text{Fe} + ^{58}\text{Ni}$  and  $^{58}\text{Ni} + ^{58}\text{Ni}$ , and  $^{58}\text{Fe} + ^{58}\text{Fe}$  and  $^{58}\text{Ni} + ^{58}\text{Ni}$ , at beam energies of 30, 40 and 47 MeV/nucleon. The details of the measurements and the extraction of isoscaling parameter can be found in Ref. [11].

Fig. 1(a) shows the experimentally obtained isoscaling parameter  $\alpha$  (symbols),

as a function of excitation energy for the Fe + Fe and Ni + Ni pair (inverted triangles), and the Fe + Fe and Fe + Ni pair (solid circles), of reactions. The excitation energy of the multifragmenting source for each beam energy was determined by simulating the initial stage of the collision dynamics using the Boltzmann-Nordheim-Vlasov (BNV) model calculation [17]. The results were obtained at a time around 40 - 50 fm/c after the projectile had fused with the target nuclei and the quadrupole moment of the nucleon coordinates (used for identification of the deformation of the system) approached zero. These excitation energies were compared with those obtained from the systematic calorimetric measurements (see Ref. [8]) for systems with mass ( $A \sim 100$ ) similar to those studied in the present work, and were found to be in good agreement with each other. One observes from the figure that there is a systematic decrease in the absolute value of the isoscaling parameter with increasing excitation energy for both pair of reactions. In addition, the  $\alpha$  parameter for the  $^{58}\text{Fe} + ^{58}\text{Fe}$  and  $^{58}\text{Ni} + ^{58}\text{Ni}$  is about twice as large compared to the one for the  $^{58}\text{Fe} + ^{58}\text{Ni}$  and  $^{58}\text{Ni} + ^{58}\text{Ni}$  pair of reactions.

Fig. 1(a) also shows a comparison between the Statistical Multifragmentation Model (SMM) [5,18] predicted isoscaling parameter (curves), and the experimentally determined isoscaling parameter for the two pairs of systems. The dashed curves in the figure correspond to the SMM calculated isoscaling parameter for the primary fragments, and the solid curves to the same for the secondary fragments. The width in the curve is the measure of the uncertainty in the inputs to the calculation. The initial parameters such as, the mass, charge and excitation energy of the fragmenting source for the SMM calculation, were obtained from the BNV calculations as discussed above. To account for the possible uncertainties in the source parameters due to the loss of nucleons during pre-equilibrium emission, the calculations were also carried out for smaller source sizes. The break-up density in the calculation was taken to be multiplicity-dependent and was varied from approximately 1/2 to 1/3 the saturation density. This was achieved by varying the free volume with the excitation energy as described in Ref. [5]. The form of the variation adopted was taken from the work of Bondorf *et al.*, [6,19] (and shown by the solid curve in Fig. 1(d)). From the above comparison, one observes that the experimentally observed decrease in the  $\alpha$  with increasing excitation energy and decreasing isospin difference  $\Delta(Z/A)^2$  of the systems, is reproduced reasonably well by the SMM calculation.

In Fig. 1(b), is shown the temperature as a function of excitation energy (*caloric curve*) obtained from the above SMM calculation. These are shown by the solid circle and inverted triangle symbols. Also shown in the figure are the experimentally measured caloric curve data compiled by Natowitz *et al.* [8] from various measurements for the mass range studied in this work. The data from these measurements are shown collectively by solid star symbols and no distinction is made among them. It is evident from the figure that the

temperatures obtained from the SMM calculation are in good agreement with the overall experimental trend in the caloric curve. By allowing the break-up density to evolve with the excitation energy, a near plateau that agrees with the experimentally measured caloric curves is thereby obtained.

The symmetry energy in the statistical model calculations is related to the isoscaling parameter through the relation [7,15,16],

$$\alpha^{prim} = \frac{4C_{sym}}{T} [(Z/A)_1^2 - (Z/A)_2^2] \quad (2)$$

where  $\alpha^{prim}$ , is the isoscaling parameter for the primary (hot) fragments, *i.e.*, before they sequentially decay into secondary (cold) fragments.  $Z_1$ ,  $A_1$  and  $Z_2$ ,  $A_2$  are the charge and the mass numbers of the composite systems from reactions 1 and 2, respectively.  $T$  is the common temperature of the systems and  $C_{sym}$  is the symmetry energy. In the above equation, the entropic contribution to the symmetry free energy is assumed to be small (the contribution becomes important at densities below  $0.008 \text{ fm}^{-3}$  [20]), the symmetry energy can therefore be substituted for the free energy. The symmetry energy in the calculation was varied until a reasonable agreement between the calculated  $\alpha$  for the secondary fragments and the measured  $\alpha$ , as shown in Fig. 1(a), was obtained.

The symmetry energy thus obtained is shown in Fig. 1(c) as a function of excitation energy. A steady decrease in the symmetry energy with increasing excitation energy is observed for both pairs of systems. The effect of the symmetry energy evolving during the sequential de-excitation of the primary fragments [12] was also estimated, and these are reflected in the large error bars shown in Fig. 1(c).

In a recent schematic calculation by Sobotka *et al.* [21], and a fully microscopic calculation by De *et al* [22], it has been shown that the plateau in the caloric curve could be a consequence of the thermal expansion of the system at higher excitation energy and decreasing density. By assuming that the decrease in the break-up density, as taken in the present statistical multifragmentation calculation, can be approximated by the expanding Fermi gas model, and the temperature in Eq. 2 and the temperature in the Fermi-gas relation are related, one can extract the density as a function of excitation energy using the simple relation,

$$T = \sqrt{K_o(\rho/\rho_o)^{2/3} E^*} \quad (3)$$

In the above expression, the momentum and the frequency dependent factors in the effective mass ratio are assumed to be one, as is to be expected for high excitation energies and low densities studied in this work [23,24].

Using the temperatures obtained from the SMM calculation and assuming  $K_o = 10$  in Eq. 3, the densities obtained as a function of excitation energy for the two pairs of systems are shown in Fig. 1(d) (solid circles and inverted triangle symbols). For comparison, we also show the break-up densities obtained from the analysis of the apparent level density parameters required to fit the measured caloric curve by Natowitz *et al.* [9]. One observes that the present results obtained by requiring to fit the measured isoscaling parameters and the caloric curve are in good agreement with those obtained by Natowitz *et al.* To verify the validity of Eq. 3, the caloric curve obtained using the above densities and excitation energies, is shown by the dotted curve in Fig. 1(b). The small discrepancy between the dashed curve and the data (solid stars) below 4 MeV/nucleon is due to the approximate nature of the Eq. 3 being used.

From figures, 1(a), 1(b), 1(c) and 1(d), one observes that the decrease in the experimental isoscaling parameter  $\alpha$ , the flattening of the temperature, the decrease in the symmetry energy and the break-up density, with increasing excitation energy are all correlated. It can thus be concluded that the expansion of the system with excitation energy during the multifragmentation process, leads to a decrease in the isoscaling parameter, symmetry energy, density, and the flattening of the temperature.

Since the temperature in the present work remains nearly constant for the range of excitation energy studied, the observed decrease in the symmetry energy with increasing excitation energy must be a consequence of decreasing density, rather than the increasing temperature.

The decrease in the symmetry energy with increasing excitation energy observed is in close agreement with the recently reported calculation of Samaddar *et al* [25]. This microscopic calculation is based on the Thomas-Fermi formulation that accounts for thermal and expansion effects in finite nuclei. Fig. 2 (second panel from the top) shows a comparison between the symmetry energy obtained from the present study and those from the Thomas-Fermi calculation. The solid circle and inverted triangle symbols correspond to the symmetry energy obtained from the present study. The solid squares correspond to the data measured in a previous study [26] at lower excitation energies. The solid blue curve is the Thomas-Fermi calculation. One observes a reasonably good agreement between the experimentally determined and the theoretically calculated symmetry energy over a broad range of excitation energy.

As mentioned earlier, the symmetry energy of finite nuclei at saturation density is often extracted by fitting ground state masses with various versions of the liquid drop mass formula. To this end, one needs to decompose the symmetry term of liquid drop into bulk (volume) and surface terms along the lines of the liquid droplet model, and identify the volume symmetry energy

coefficient as the symmetry energy derived from infinite nuclear matter at saturation density. Recently, there have been numerous efforts [27] to constrain the density dependence of the symmetry energy of infinite nuclear matter. Following the expression for the symmetry energy of finite nuclei at normal nuclear density by Danielewicz [28], and using the constraint obtained from recent work on the the symmetry energy of infinite nuclear matter, one can empirically write the symmetry energy of a finite nucleus of mass  $A$ , as,

$$S_A(\rho) = \frac{\alpha(\rho/\rho_0)^\gamma}{1 + [\alpha(\rho/\rho_0)^\gamma/\beta A^{1/3}]} \quad (4)$$

where,  $\alpha = 31 - 33$  MeV,  $\gamma = 0.55 - 0.69$  and  $\alpha/\beta = 2.6 - 3.0$ . The quantities  $\alpha$  and  $\beta$  are the volume and the surface symmetry energy at normal nuclear density. At present, the values of  $\alpha$ ,  $\gamma$  and  $\alpha/\beta$  remain unconstrained. The ratio of the volume symmetry energy to the surface symmetry energy ( $\alpha/\beta$ ), is closely related to the neutron skin thickness [28]. Depending upon how the nuclear surface and the Coulomb contribution is treated, two different correlations between the volume and the surface symmetry energy have been predicted [3] from fits to nuclear masses. Experimental masses and neutron skin thickness measurements for nuclei with  $N/Z > 1$  should provide tighter constraint on the above parameters.

To compare the above empirical relation with the Thomas-Fermi calculation, we have assumed in Eq. 4 the same excitation energy dependence of the density of the expanding nucleus as obtained from the Thomas-Fermi calculation. The assumed excitation energy dependence of the density are shown by solid curves in the bottom most panel of Fig. 2 for nuclear masses of  $A = 40, 150$  and  $197$ . For comparison, we also show in this plot the densities obtained from the present study (solid circles and inverted triangles) and those from Ref. [9] (star symbols). The results of the empirical relation, Eq. 4, with  $\alpha = 31.6$  MeV,  $\gamma = 0.69$  and  $\alpha/\beta = 2.6$ , are shown by the dashed curves in top three panels of Fig. 2 for  $A = 40, 150$  and  $197$ . It is observed that the symmetry energy determined from the empirical relation (dashed curve) compares very well with the more formal Thomas-Fermi calculation (solid curve). The numerical values obtained from Eq. 4 agrees very well over a wide range of nuclear mass and excitation energy. Future measurements of symmetry energy as a function of excitation energy for very light and heavy nuclei should provide further insight into the validity and the theoretical understanding of the empirical relation and the Thomas-Fermi formalism.

In summary, the excitation energy dependence of the symmetry energy in multifragmentation reactions of  $^{58}\text{Ni} + ^{58}\text{Ni}$ ,  $^{58}\text{Fe} + ^{58}\text{Ni}$  and  $^{58}\text{Fe} + ^{58}\text{Fe}$  systems is studied. It is observed that the symmetry energy of a highly excited system decrease with increasing excitation energy. The decrease is mainly due to the expansion that the system undergoes as its excitation energy increases.

A comparison of the experimental data with the microscopic Thomas-Fermi calculation that accounts for the thermal and expansion effects in finite nuclei, shows good agreement. An empirical relation that can be used to study the symmetry energy of finite nuclei in various mass region is thereby proposed.

We thank Drs. J.N. De and S.K. Samaddar for making us available the results of their Thomas-Fermi calculation. We also thank Dr. J.B. Natowitz for providing us the data points from his studies on break-up density and caloric curve. This work was supported in part by the Robert A. Welch Foundation through grant No. A-1266, and the Department of Energy through grant No. DE-FG03-93ER40773.

## References

- [1] J.R. Stone and P.G. Reinhard, *Prog. Part. Nucl. Phys.* 58 (2007) 587.
- [2] D. Lunney, J.M. Pearson, and C. Thibault, *Rev. Mod. Phys.* 75, (2003) 1021.
- [3] A.W. Steiner, M. Prakash, J.M. Lattimer, and P.J. Ellis, *Phys. Rep.* 411, (2005) 325.
- [4] B.A. Brown, *Phys. Rev. Lett.* 85 (2000) 5296.
- [5] J.P. Bondorf, A.S. Botvina, A.S. Iljinov, I.N. Mishustin and K. Sneppen, *Phys. Rep.* 257, (1995) 133.
- [6] J.P. Bondorf, R. Donangelo, I.N. Mishustin and H. Schultz, *Nucl. Phys. A* 444, (1985) 460.
- [7] A.S. Botvina, O.V. Lozhkin, and W. Trautmann, *Phys. Rev. C* 65, (2002) 044610.
- [8] J.B. Natowitz, R. Wada, K. Hagel, T. Keutgen, M. Murray, A. Makeev, L. Qin, P. Smith, and C. Hamilton, *Phys. Rev. C* 65, (2002) 034618; *and references therein.*
- [9] J.B. Natowitz, K. Hagel, Y. Ma, M. Murray, L. Qin, S. Shlomo, R. Wada, and J. Wang, *Phys. Rev. C* 66, (2002) 031601.
- [10] V.E. Viola, K. Kwiatkowski, J.B. Natowitz, and S.J. Yennello, *Phys. Rev. Lett.* 93, (2004) 132701.
- [11] D.V. Shetty, S.J. Yennello, A.S. Botvina, G.A. Souliotis, M. Jandel, E. Bell, A. Keksis, S. Soisson, B. Stein and J. Igljo, *Phys. Rev. C* 70, (2004) 011601.
- [12] J. Igljo, D.V. Shetty, S.J. Yennello, G.A. Souliotis, M. Jandel, A. Keksis, S. Soisson, B. Stein and S. Wuenschel, *Phys. Rev. C* 74, (2006) 024605.
- [13] A. LeFevre *et al.*, *Phys. Rev. Lett.* 94, (2005) 162701.

- [14] D. Henzlova, A.S. Botvina, K.H. Schmidt, V. Henzl, P. Napolitani, M.V. Ricciardi, nucl-ex/0507003 (2005).
- [15] M.B. Tsang *et al.*, Phys. Rev. C 64, (2001) 054615.
- [16] M.B. Tsang *et al.*, Phys. Rev. Lett. 86, (2001) 5023.
- [17] V. Baran, M. Colonna, M. Di Toro, V. Greco, M. Zielinska-Pfabe and H.H. Wolter, Nucl. Phys. A 703, (2002) 603.
- [18] A.S. Botvina and I.N. Mishustin, Phys. Rev. C 63, (2001) 061601.
- [19] J.P. Bondorf, A.S. Botvina and I.N. Mishustin, Phys. Rev. C 58, (1998) 27.
- [20] C.J. Horowitz and A. Schwenk, Nucl. Phys. A 776 (2006) 55.
- [21] L.G. Sobotka, R.J. Charity, J. Toke and W.U. Schroder, Phys. Rev. Lett. 93, (2004) 132702.
- [22] J.N. De, S.K. Samaddar, X. Vinas and M. Centelles, Phys. Lett. B 638, (2006) 160.
- [23] R. Hasse and P. Schuck, Phys. Lett. B 179, (1986) 313.
- [24] S. Shlomo and J.B. Natowitz, Phys. Lett. B 252, (1990) 187; Phys. Rev. C 44, (1991) 2878.
- [25] S.K. Samaddar, J.N. De, X. Vinas, and M. Centelles, Phys. Rev. C 76, (2007) 041602.
- [26] G.A. Souliotis *et al.*, Phys. Rev. C 73, (2006) 024606; Phys. Rev. C 75, (2007) 011601.
- [27] D.V. Shetty, S.J. Yennello and G.A. Souliotis, Phys. Rev. C 75 (2007) 034602; *and references therein.*
- [28] P. Danielewicz, Nucl. Phys. A 727, (2003) 233.

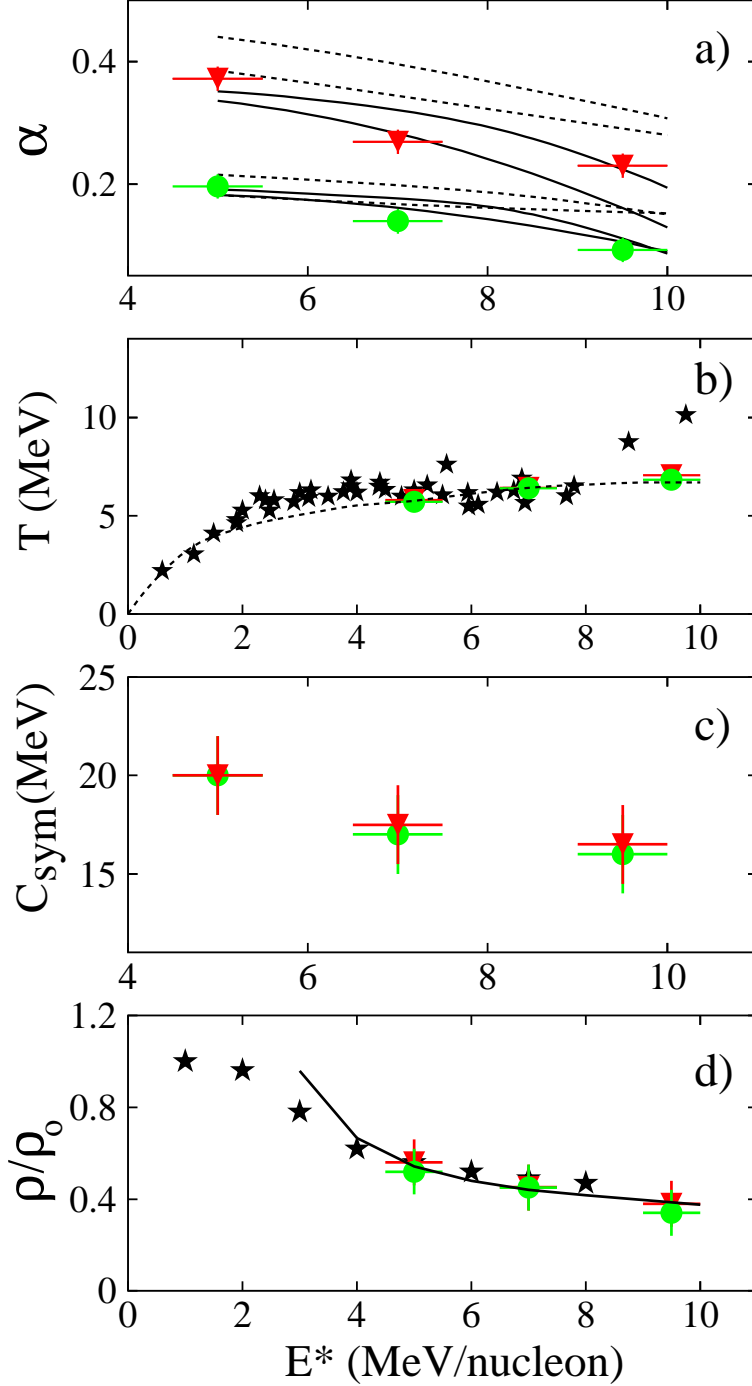


Fig. 1. (Color online) Isoscaling parameter  $\alpha$ , temperature  $T$ , symmetry energy  $C_{sym}$ , and density as a function of excitation energy for the Fe + Fe and Ni + Ni pair of reaction (inverted triangles), and Fe + Ni and Ni + Ni pair of reactions (solid circles) for the 30, 40 and 47 MeV/nucleon. a) Experimental isoscaling parameter as a function of excitation energy. The solid and the dashed curves are the SMM calculations as discussed in the text. b) Temperature as a function of excitation energy. The solid stars are taken from Ref. [8]. The dashed curve corresponds to the one determined from Eq. 3. c) Symmetry energy as a function of excitation energy. d) Density as a function of excitation energy. The solid stars are from Ref. [9]. The solid curve is from Ref. [6].

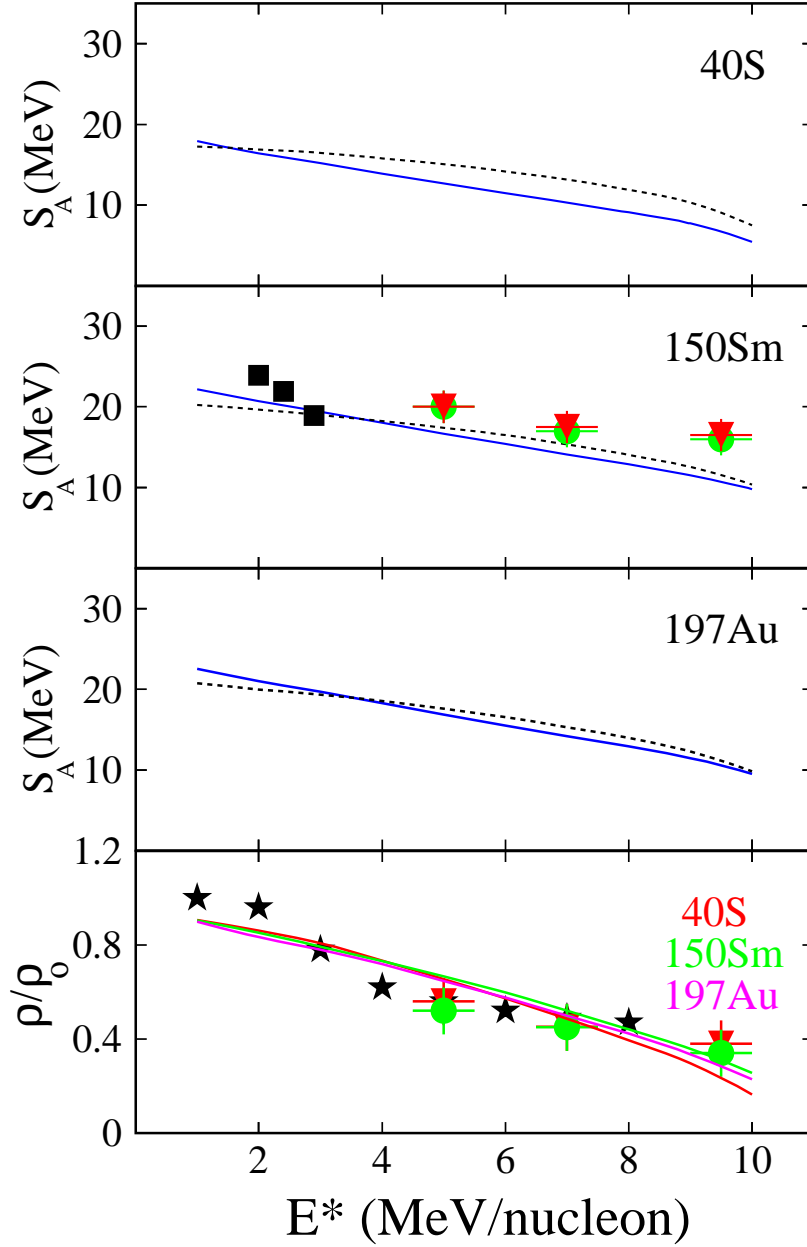


Fig. 2. (Color online) Top three panels: Symmetry energy as a function of excitation energy for  $A = 40, 150$  and  $197$ . The solid blue curve corresponds to the Thomas-Fermi calculation and the dotted curve to the empirical relation Eq. 4 as discussed in the text. Bottom panel: Density as a function of excitation energy. The curves are from the Thomas-Fermi calculation. The star symbols are data from Ref. [8]. The solid circle and inverted triangle symbols are from the present study.